The Journal of Korean Vacuum Science & Technology
Vol. 2, No. 2, October 1998, pp. 92~96

Preparation of ferroelectric $SrBi_2Ta_2O_9$ thin films deposited by multi-target sputtering

Cheol-Hoon Yang and Soon-Gil Yoon

Dept. of Materials Engineering, Chungnam National University,
Daeduk Science Town, 305-764, Taejon, Korea

(Received March 5, 1998)

Abstract – Ferroelectric Bi-layered oxides $SrBi_2Ta_2O_9$ (SBT) thin films have been deposited on Pt/Ti/SiO_2/Si substrates using multi-target sputtering. Structure, composition, and electrical properties have been investigated on films. The SBT films were deposited with the various bismuth sputtering powers. The SBT films deposited with the bismuth sputtering power of 20 W have the most dense microstructure and the remanent polarization (P_r) of 9.2 $\mu C/cm^2$ and the coercive field (E_c) of 43.8 kV/cm at an applied voltage of 5 V. The SBT films deposited with the bismuth sputtering power of 20 W showed a fatigue-free characteristics up to 1.0×10^{10} cycles under 5 V bipolar pulse and a leakage current density of 2.0×10^{-8} A/cm^2 at 200 kV/cm.

I. Introduction

Recently, there is a great interest in the application of ferroelectric thin films in nonvolatile memories [1-4]. Strontium bismuth tantalate, $SrBi_2Ta_2O_9$, has attracted great interest as a promising ferroelectric material for application to storage capacitors in nonvolatile ferroelectric random access memories, because of its nonfatigue nature and possibility of low polarization switching voltage [5-6]. The capacitors formed by Bi layered $SrBi_2Ta_2O_9$ show no significant fatigue after 10^{12} switching cycles [7-8]. However, the remanent polarization of SBT is not high enough for high-density memories; this problem is ever more serious when the temperature dependence of the remanent polarization is considered [9]. Ferroelectric properties of the SBT films were greatly dependent on the composition of the films. Atsuki *et al.* [10] reported that Sr-deficient sol-gel films prepared at 800°C yielded higher remanent polarization values than the films with stoichiometric Sr/Ta atomic ratio.

SBT ferroelectric films have been synthesized mainly by metalorganic-decomposition (MOD) [11, 12], pulsed laser ablation deposition (PLD) [13], metalorganic chemical vapor deposition (MOCVD) [14], and rf magnetron sputtering technique [15, 16]. When the SBT films were deposited using the single target, bismuth content in SBT films was difficult to control because bismuth content in SBT films was very sensitive to the deposition conditions such as sputtering pressure and sputtering gas ratio. Therefore, in this study, a modified rf magnetron sputtering system was used to easily control the bismuth content in SBT films. The structural and ferroelectric properties of SBT films prepared by multi-target sputtering system were evaluated.

II. Experimental Details

The SBT target was processed by mixing $SrCO_3$, Bi_2O_3 and Ta_2O_5 powders by ball mill, calcining the mixed powders at 1000°C, and then pressing the calcined powders in a circular die of 2 inch diameter. The pressed target was sintered for 1 h at 1000°C in the air ambient. The composition of the target was a $Sr_{1.2}Bi_{2.4}Ta_{2.0}O_9$ ceramic with 20 and 20 mole % excess $SrCO_3$ and Bi

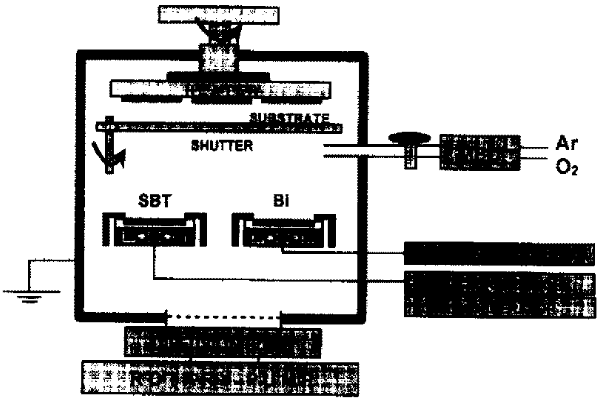

Fig. 1. Schematic diagram of a modified rf magnetron sputtering equipment for preparation of the SBT thin films.

$_2O_3$ to compensate for the deficiency of Sr and Bi in SBT films, respectively. Though the target has the Bi excess, Bi content in SBT film was still deficient. Therefore, Bi target was used simultaneously with the SBT target to compensate for the deficiency of Bi in SBT films. Multi-target sputtering system used in this study was illustrated schematically in Fig. 1.

The Pt(150 nm)/Ti(100 nm)/SiO_2(450 nm)/Si (001) substrates were purchased from Silicon Quest International Incorporated (SQI).

After pumping down the sputtering chamber to a base pressure of 1.2×10^{-5} torr, argon and oxygen mixtures were introduced into the sputtering chamber and controlled with a mass flow controller. The deposition pressure was changed by controlling the main valve between the pump and the deposition chamber. The detailed sputtering conditions of SBT thin films are summarized in Table 1. The SBT films were deposited using the SBT and Bi targets at 500°C and then annealed at 800°C for 1 h in an oxygen ambient.

The crystal structure of the films was characterized by X-ray diffraction (XRD) employing Cu$K\alpha$ radiation and a Ni filter. The morphology and the thickness of the deposited SBT films were determined with a scanning electron microscope (SEM). The composition of SBT films was determined by electron probe micro-analyzer (EPMA).

Table 1. Typical sputtering conditions of SBT thin films

Target material	Sintered $Sr_{1.2}Bi_{2.4}Ta_{2.0}O_9$ and Bi
Substrate	Pt/Ti/SiO_2/Si
Target diameter	5.08 cm
Base pressure of system	1.2×10^{-5} Torr
Sputtering pressure	10 mTorr
RF sputtering power	100 W
Bi sputtering power	10, 20, 30, and 40 W
Sputtering gas (Ar : O_2)	1 : 1
Substrate temperature	500°C
Annealing temperature	800°C for 1 h (in O_2 ambient)

For electrical measurements, top electrodes of platinum (80 nm thickness and 100 μm diameter) were deposited by dc sputtering using a shadow mask. Ferroelectric properties (polarization vs. electric field, and fatigue property) were measured using a RT 66A ferroelectric tester (Radient Technology) operating in the virtual ground mode. The current-voltage (I-V) measurements were performed with a Keithley 617 programmable electrometer. The leakage current behavior was determined with a voltage step of 0.1 V and delay time of 1 s.

3. Results and Discussion

Fig. 2 shows the X-ray diffraction patterns of SBT films deposited with the various bismuth sputtering powers. The main peaks of (115) and (200) were shown at the SBT films deposited at various bismuth sputtering powers. However, BTO ($Bi_4Ti_3O_{12}$) peak intensity at about 2θ=30° increases with increasing the bismuth sputtering power. This peak was differently indexed with (107) of SBT film by Song *et al.* [14] and Bi_2Pt phase by Atsuki *et al.* [9]. It is very important to index correctly because this peak might be indicated another phases. Titanium diffused through the Pt layer of Pt/Ti/SiO_2/Si was reacted with the bismuth and the oxygen during the deposition of the SBT films, and thus the $Bi_4Ti_3O_{12}$ phase could form. Therefore, the peak intensity of the BTO increases with increasing

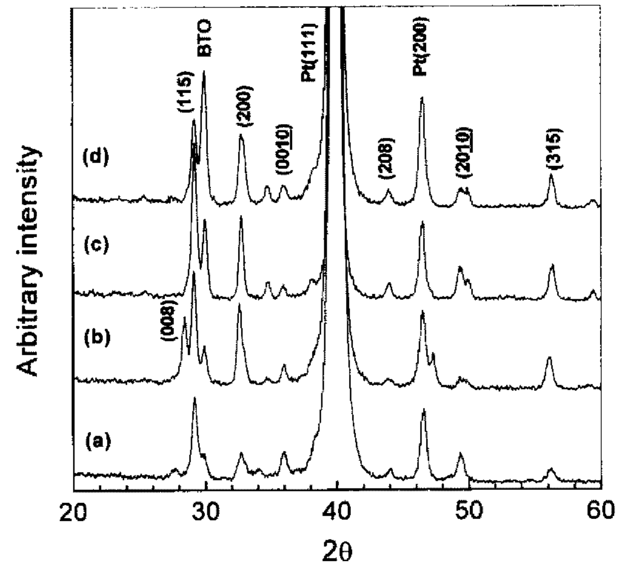

Fig. 2. X-ray diffraction patterns of the SBT films deposited on Pt/Ti/SiO$_2$/Si substrates with the bismuth sputtering powers of (a) 10, (b) 20, (c) 30, and (d) 40 W.

the bismuth contents as shown in Fig. 2. These BTO phases might affect the electrical properties of the SBT films [16].

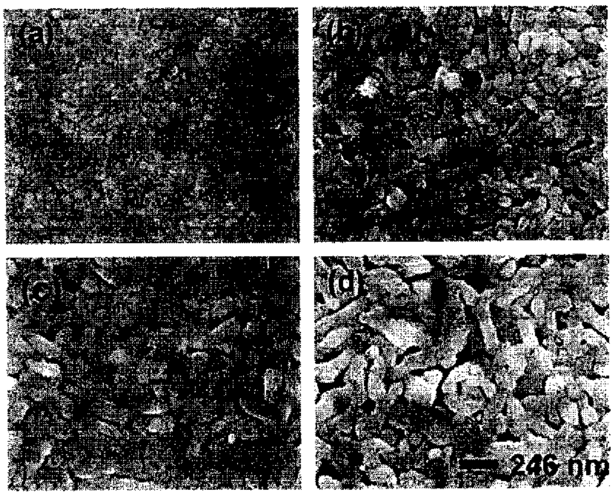

Fig. 3. SEM surface images of the SBT films deposited with the bismuth sputtering powers of (a) 10, (b) 20, (c) 30, and (d) 40 W.

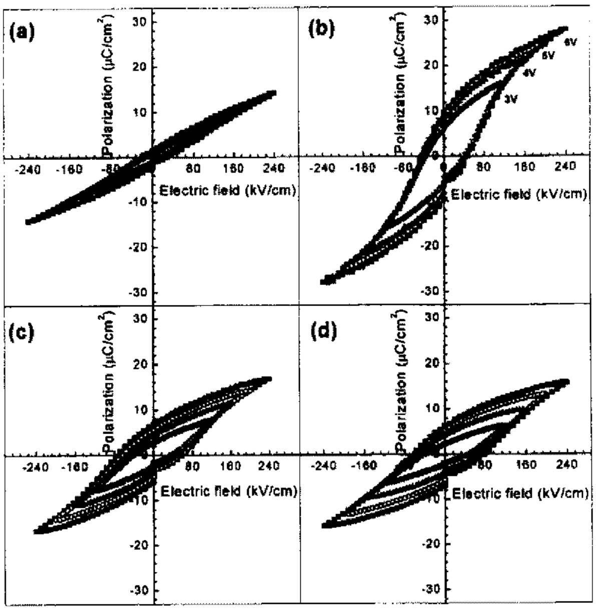

Fig. 4. Hysteresis loops of the SBT films deposited with the bismuth sputtering powers of (a) 10, (b) 20, (c) 30, and (d) 40 W.

Fig. 3 shows the SEM surface images of SBT films deposited with the various bismuth sputtering powers. The grain size of the SBT films increases with increasing the bismuth sputtering powers. The SBT films deposited with the bismuth sputtering power of 40 W showed a porous microstructure. The SBT films deposited with 20 W showed the most dense microstructure. Hysteresis loops of SBT films deposited with the various bismuth sputtering powers were shown in Fig. 4. The SBT films deposited with the bismuth sputtering power of 10 W had a low remanent polarization and coercive field and did not show a complete loop. However, hysteresis loop of the SBT films deposited with 20 W show a shape saturated at 3 V and a remanent polarization of 9.2 μC/cm^2 and a coercive field of 43.8 kV/cm at the excitation voltage of 5 V. The hysteresis loop of SBT films deposited with bismuth sputtering power above 20 W show a lower remanent polarization and higher coercive field than that of bismuth sputtering power 20 W. These results suggested that microstructure, morphology, and the composition of SBT film affected the ferroelectric properties of the films. The variation of the composition of SBT films as a function of bismuth sputtering power was shown in Fig. 5. The bismuth content of the SBT films monotonously increases with increasing the bismuth sputtering power and strontium content was kept at almost constant value with increasing

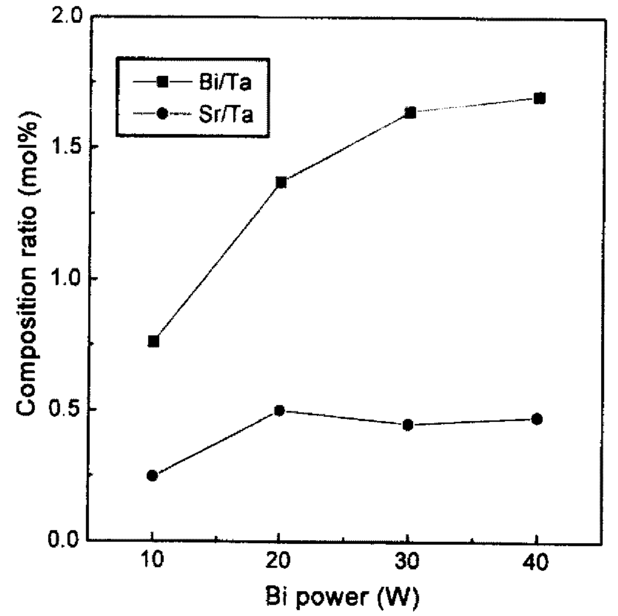

Fig. 5. The composition of the SBT films as a function of bismuth sputtering powers.

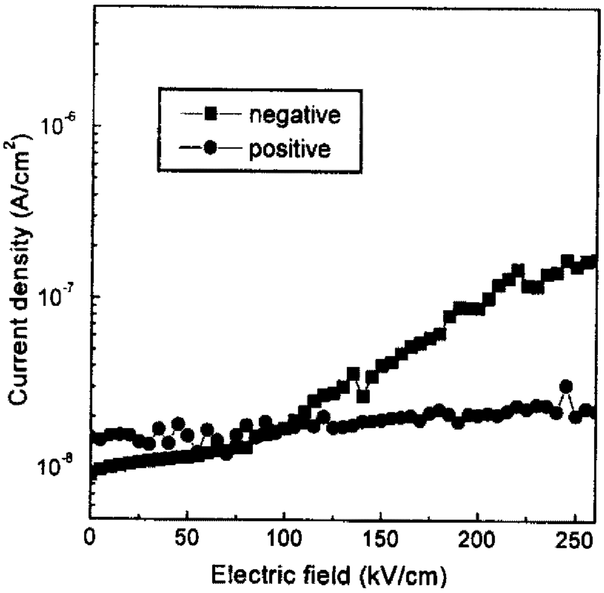

Fig. 7. Leakage current characteristics of the SBT films deposited with the bismuth sputtering power of 20 W.

the bismuth sputtering power. The composition of the SBT films deposited with the bismuth sputtering power of 20 W was about Sr, 1.0; Bi, 2.7; Ta, 2.0.

Fatigue characteristics of the SBT films deposited with the bismuth sputtering power of 20 W at room temperature were shown in Fig. 6. Fatigue test was done using a 5 V bipolar square pulses at 1 MHz produced by function generator.

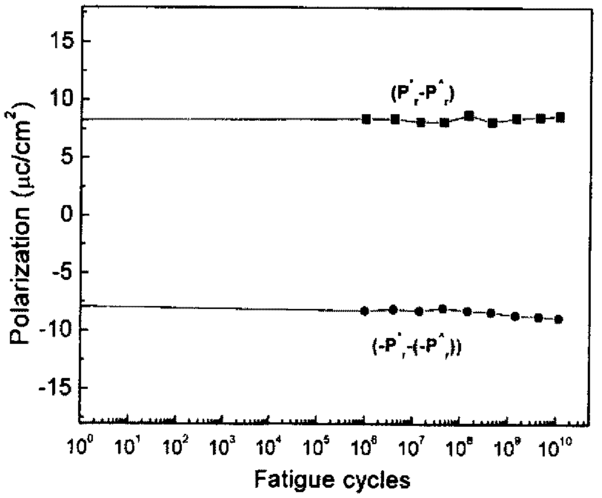

Fig. 6. Fatigue characteristics of the SBT films deposited with the bismuth sputtering power of 20 W [P^*_r; $P_s(V_{max})$-$P_r(-V_{max})$, $P^\wedge_r$; $P_s(V_{max})$-$P_r(V_{max})$, $-P^*_r$; $P_s(-V_{max})$-$P_r(V_{max})$, $-P^\wedge_r$; $P_s(-V_{max})$-$P_r(-V_{max})$].

In this plots, (P^*_r-$P^\wedge_r$) indicates a practical polarization used in nonvolatile memories. In Fig. 6, the films show practically no polarization fatigue up to 1.0×10^{10} switching cycles at room temperature and the films could meet the criteria for consumer applications of nonvolatile memory devices. The sputtered SBT films have very good fatigue characteristics.

The leakage current characteristics of a 250 nm thick SBT films deposited with bismuth sputtering power of 20 W was shown in Fig. 7. The leakage current density shows almost constant value of 1.0×10^{-8} A/cm^2 with increasing applied electric field. The leakage current of SBT films deposited on Pt/Ti/SiO_2/Si substrates always shows the lower value by one order of magnitude than that of SBT films deposited on Pt/SiO_2/Si substrates [17]. The reason for this result was due to the influence of BTO phase formed at the interface between SBT and Pt/Ti/SiO_2/Si substrate. The leakage current characteristics of the SBT films deposited on Pt / Ti / SiO_2 / Si substrates were controlled by the Schottky emission from the previous experimental results [9]. Because Schottky emission was controlled by the interface between the electrode and the SBT films, the BTO layer formed at the interface between the bottom electrode and the SBT films could increase the Schottky barrier height and thus decreased the leakage current density of the SBT films.

IV. Conclusions

Ferroelectric Bi-layered oxide $SrBi_2Ta_2O_9$ thin films were successfully deposited on Pt/Ti/SiO_2/Si substrates by sputtering using a sintered $Sr_{1.2}Bi_{2.4}Ta_{2.0}O_9$ ceramic target and a Bi metal target. The bismuth content in the SBT films could be easily controlled using the multi-targets. The $Sr_{1.0}Bi_{2.7}Ta_{2.0}O_9$ films deposited with the bismuth sputtering power of 20 W have the most dense microstructure and the remanent polarization P_r of 9.2 $\mu C/cm^2$ and the coercive field E_c of 43.8 kV/cm at an applied voltage of 5 V. The second phase, like $Bi_4Ti_3O_{12}$, was formed at the interface between the bottom electrode and the SBT films. The SBT films deposited with the bismuth sputtering power of 20 W showed a fatigue-free characteristics up to 1.0×10^{10} cycles under 5 V bipolar pulse and a leakage current density of 2.0×10^{-8} A/cm^2 at 200 kV/cm. The SBT films deposited by multi-target sputtering are attractive for the application to nonvolatile memory devices.

References

1. W. A. Geidemand, IEEE trans. Ultrason. Ferroelectr. Freq. Control. **38**, 705 (1991).
2. J. F. Scott and C. A. Araujo, Science **246**, 1400 (1989).
3. J. F. Scott, C. A. Araujo, and L. D. McMillan, Proc. Ultrason. Symp., 229 (1980).
4. S. S. Eaton, D. B. Butler, M. Parris, D. Wilson, and H. McNellie, Proc. IEEE Int. Solid state Circuit Conf., 130 (1988).
5. C. A. Paz de Araujo, L. D. McMillan, J. D. Cuchiaro, and M. C. Scott and M. C. Scott, Nature **374**, 627 (1995).
6. K. Amanum, T. Hase, and Y. Miyasaka, Appl. Phys. Lett. **66**, 9 (1995).
7. C. A. Paz de Araujo, L. D. McMillan, J. D. Cuchiaro, and M. C. Scott, International Patent Application WO 93/12542 (1993).
8. T. Mihara, H. Watanabe, C. A. Paz de Araujo, L. D. McMillan, J. D. Cuchiaro, and M. C. Scott, Pro. Fourth Int. Symp. Integrated Ferroelectrics, p. 137 (1992).
9. C. H. Yang, S. S. Park, and S. G. Yoon, J. Electrochem. Soc. **145**, 1330 (1998).
10. T. Atsuki, N. Soyama, T. Yonezawa and K. Ogi, Jpn. J. Appl. Phys. **34**, 5069 (1995).
11. K. Amanuma, T. Hase, and Y. Miyasaka, Appl. Phys. Lett. **66**, 221 (1995).
12. M. Klee, paper presented at 7th International Symposium on Integrated Ferroelectrics held in Colorado Springs, CO, March 20-22 (1995).
13. R. Dat, J. K. Lee, O. Auciello, and A. I. Kingon, Appl. Phys. Lett. **67**, 572 (1995).
14. T. Li, Y. Zhu, Y. Zhu, S. B. Desu, C. H. Peng, and M. Nagata, Appl. Phys. Lett. **68**, 616 (1996).
15. T. K. Song, J. K. Lee, and H. J. Jung, Appl. Phys. Lett. **69**, 3839 (1996).
16. S. S. Park, C. H. Yang, and S. G. Yoon, J. Electrochem. Soc. **144**, 2855 (1997).
17. N. J. Seong, Cheol-Hoon Yang, Woong-Chul Shin, and S. G. Yoon, Appl. Phys. Lett. **72** (1998), to be published.